



# Modeling COVID-19 Pandemic with Hierarchical Quarantine and Time Delay

Wei Yang<sup>1</sup>

Accepted: 10 March 2021 / Published online: 24 March 2021

© The Author(s), under exclusive licence to Springer Science+Business Media, LLC, part of Springer Nature 2021

## Abstract

COVID-19 comes out as a sudden pandemic disease within human population. The pandemic dynamics of COVID-19 needs to be studied in detail. A pandemic model with hierarchical quarantine and time delay is proposed in this paper. In the COVID-19 case, the virus incubation period and the antibody failure will cause the time delay and reinfection, respectively, and the hierarchical quarantine strategy includes home isolation and quarantine in hospital. These factors that affect the spread of COVID-19 are well considered and analyzed in the model. The stability of the equilibrium and the nonlinear dynamics is studied as well. The threshold value  $\tau_k$  of the bifurcation is deduced and quantitatively analyzed. Numerical simulations are performed to establish the analytical results with suitable examples. The research reveals that the COVID-19 outbreak may recur over a period of time, which can be helpful to increase the number of tested people with or without symptoms in order to be able to early identify the clusters of infection. And before the effective vaccine is successfully developed, the hierarchical quarantine strategy is currently the best way to prevent the spread of this pandemic.

**Keywords** COVID-19 · Pandemic model · Hierarchical quarantine · Time delay · Bifurcation

## 1 Introduction

According to the report of the World Health Organization (WHO), as of June 14, 2020, there have been a total of 7.855 million confirmed cases of coronavirus disease 2019 (COVID-19) across the globe. The outbreak of COVID-19 which is ravaging globally has severely affected the safety and the development around the world. The history of human coronavirus began in 1965 when a virus named B814 was found by Tyrrell [1]. Since 2003, at least five new human coronaviruses have been identified (such as the SARS pandemic and H1N1 influenza in 2009), which caused significant morbidity and mortality. On February 11, 2020, the WHO announced that the disease caused by this new coronavirus was a COVID-19 [2]. It concluded that the virus can be transmitted from human-to-human.

---

✉ Wei Yang  
yangwei@mail.neu.edu.cn

<sup>1</sup> Software College, Northeastern University, Shenyang 110169, China

Symptomatic people are the most common source of COVID-19 spreading, however, the possibility of transmission before the onset of symptoms cannot be excluded.

The propagation rules and predictions of various infectious diseases require theoretical analysis, quantitative analysis and simulations. The analysis is inseparable from the mathematical model established for various infectious diseases. Therefore, understanding diseases and modeling the spread of pandemic mathematically attract a lot of attention. As early as 1906, Hamer used a discrete mathematical model to study the pandemic pattern of measles [3]. In 1911, Ross established a differential equation model to study the spread of malaria [4]. In 1927, Kermack and Mckendrick established a compartment model with a bilinear incidence rate in order to analyze the spread of the Black Death in London [5]. Based on this work, many researches have studied the spread of infectious diseases in a population by compartmental models such as SIS, SIR, SIRS or SEIR [6–9]. The use of disease transmission models to generate short-term and long-term pandemic forecasts has increased as the number of infectious disease outbreaks has increased over the last decades [10]. To investigate the pandemic of COVID-19, some models have been made modifications based on the conventional “SEIR” model [11] and concluded that strictly controlled interventions are critically important to impede COVID-19 outbreak [12–17]. A few models established a stochastic transition model to evaluate the spread of COVID-19 and also emphasized the necessity for isolation and quarantine [18, 19]. Some other models have been developed to evaluate the role of coronavirus transmission based on asymptomatic cases [20, 21]. However, a crucial factor caused by asymptomatic cases or virus incubation period is not considered, that is the time delay. Because it is hard to find and confirm the infected cases in good time, there will be a time delay before the infected cases are quarantined. Then, bifurcation, chaos or fractal may occur in the pandemic dynamic system, which means the COVID-19 pandemic may outbreak over and over again. It will cause great difficulties to the prevention and control of the COVID-19 outbreak. Kissler et al. have given a similar projection by using estimates of seasonality, immunity and cross-immunity, that is, the recurrent wintertime outbreaks of COVID-19 will probably occur after the initial, most severe pandemic wave [46].

The study of complex dynamic evolutionary behavior of nonlinear dynamical systems may cover ecology, economics, computer science and many other fields. Li et al. discuss bifurcation and chaos of the discrete model about a physiological control system with delay [22]. The qualitative analysis of the discrete model including the boundedness of solutions and bifurcation is investigated in [23]. In order to reveal the effect of time delay on the stability and Hopf bifurcation, the fractional neural networks with delay were investigated in [24]. Dong et al. proposed a computer virus model with time delay, and they regard the time delay as bifurcating parameter to study the dynamical behaviors including Hopf bifurcation and local asymptotical stability [25]. Other studies in computer science show that the spread dynamic system of malware would be unstable and appear bifurcation and chaos [26–28]. These studies illustrate that time delay will cause unpredictable and complex influence on the dynamic system. This paper aims to analyze the impact caused by time delay on the dynamic of COVID-19 spreading and the effect of home isolation, hospital isolation, antibody failure and other factors on the pandemic prevention and control. We try to provide some suggestions to more effectively prevent the spread of COVID-19 through feasible measures.

This paper is organized as follows. In Sect. 2, I propose the SIDQR pandemic model with hierarchical quarantine and time delay. Section 3 analyzes the stability of equilibrium and deduces the threshold of Hopf bifurcation. In Sect. 4, based on the model, I carry out the numerical simulations for the dynamics and bifurcation phenomenon of the COVID-19

outbreak. Section 5 gives the discussion about the prevention of COVID-19 and the conclusion for this paper.

## 2 Pandemic Model with Hierarchical Quarantine and Time Delay

To effectively suppress the spread of the pandemic, many governments around the world have taken measures to extend vacations and quarantine. Practice has proved that quarantine is an effective measure in large-scale pandemic situation. In order to illustrate the importance of quarantine measures to restrain the propagation of the COVID-19, I propose a nonlinear pandemic model by considering hierarchical quarantine measures and time delay.

In order to show clearly, the transition diagram and frequently used notations of the model is given in Fig. 1 as follows.

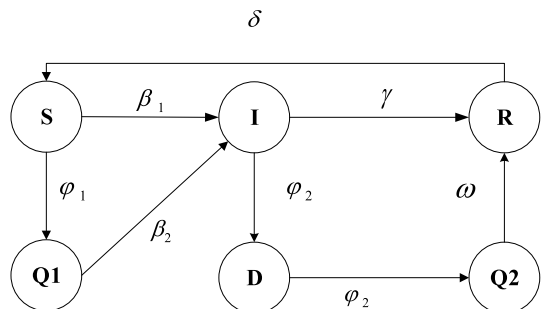
In the model, the population is partitioned into six compartments depending on the states. *Susceptible* state ( $S$ , it denotes the population who are at risk of being infected by the COVID-19). *Infected* state ( $I$ , it denotes the population who are infected by COVID-19). *Delayed* state ( $D$ , it denotes the number of delayed population. In this case, if someone is infected by COVID-19, it will take some days to get a definite diagnosis and be quarantined in a hospital setting, and this state can be regarded as a transitional state). *Home isolation* state ( $Q_1$ , it denotes the restriction of movement or isolation from the people who are susceptible to a contagious disease). *Quarantine* state ( $Q_2$ , it denotes that the confirmed patients who are quarantined in a hospital setting) and *Recovered* state ( $R$ , it denotes the population who are recovered from COVID-19). The notations and their explanations are listed as follows.

### 2.1 Some Hypotheses

In this paper, the pandemic models are based on the following hypothesis:

- (1) At every time step, the susceptible population will be infected by the infected population at a rate  $\beta_1$ , and the susceptible population will be subjected to home isolation at a rate  $\varphi_1$ . The value of  $\varphi_1$  depends on the management of the government and the degree of public compliance.
- (2) In reality, the population who is isolated at home still may be infected at a small risk, because it is unavoidable for the isolated people to contact the others. Some infected

**Fig. 1** State transition diagram of the pandemic model



cases have been confirmed to be caused by family gatherings. Thus, the population at home isolation state will be infected at a rate  $\beta_2$  in the model.

- (3) For the infected population, a small number of confirmed patients will be self-healing at a rate  $\gamma$ , others will be quarantined in a hospital at a rate  $\varphi_2$ . However, the infected population will take some days to be confirmed and quarantined in the hospital. Then, there is a delayed state between infected state and quarantine state in this case.
- (4) The quarantined population in the hospital will get recovered at a rate  $\omega$ .
- (5) Currently, there is no evidence that people can get permanent immunity, even the vaccine may be invalid after a period of time. In the model, the recovered population may be susceptible again at a rate  $\delta$ , it is inversely related to the duration of the vaccine effect.
- (6) The total number of population is assumed as  $N$ . To study the nonlinear dynamics of the pandemic model, the total number  $N$  in the system is fixed.

### 2.2 Model Formulation

Based on the hypothesis and the transition diagram of COVID-19 in human population as depicted in Fig. 1, the model can be expressed with the following equations (the source and explanations of the equations can be found in [45]):

$$\left\{ \begin{aligned} \frac{dS(t)}{dt} &= \delta R(t) - \frac{\beta_1 I(t)S(t)}{N} - \varphi_1 S(t), \\ \frac{dI(t)}{dt} &= \frac{\beta_1 I(t)S(t)}{N} + \frac{\beta_2 I(t)Q_1(t)}{N} - (\gamma + \varphi_2)I(t), \\ \frac{dD(t)}{dt} &= \varphi_2 I(t) - \varphi_2 I(t - \tau), \\ \frac{dQ_1(t)}{dt} &= \varphi_1 S(t) - \frac{\beta_2 I(t)Q_1(t)}{N}, \\ \frac{dQ_2(t)}{dt} &= \varphi_2 I(t - \tau) - \omega Q_2(t), \\ \frac{dR(t)}{dt} &= \gamma I(t) + \omega Q_2(t) - \delta R(t), \end{aligned} \right. \tag{1}$$

and the total population is:

$$N = S(t) + I(t) + D(t) + Q_1(t) + Q_2(t) + R(t) \tag{2}$$

In the model, the infection rates  $\beta_1$  and  $\beta_2$  are determined by three parameters: the successfully infecting rate of the virus (parameter  $b$ ), the number of people that a virus carrier contacts each day (parameter  $k$ ) and the average number of days that the infected population can spread the virus (parameter  $D$ ). In order to calculate the value of this parameter, I use a simplified model (*SIR* model) to fit the real data. Assuming a person is infected at the beginning of the outbreak, according to the basic epidemic *SIR* model,

$$\frac{dI(t)}{dt} = \frac{\beta_1 I(t)S(t)}{N} - \gamma I(t) \approx (\beta_1 - \gamma)I(t), \tag{3}$$

The solution of the above formula can be solved as the following equation:

**Table 1** Notations and their explanations in this paper

Notations	Explanations
$S(t)$	The number of susceptible population at time $t$
$I(t)$	The number of infected population at time $t$
$Q_1(t)$	The number of home isolation population at time $t$
$Q_2(t)$	The number of quarantine population at time $t$
$D(t)$	The number of delayed population at time $t$
$R(t)$	The number of recovered population at time $t$
$N$	The total number of population in the model
$\beta_1$	The infection rate for susceptible population
$\beta_2$	The infection rate for home isolation population
$\varphi_1$	The rate of the susceptible population compliance home isolation
$\varphi_2$	The rate of the infected population that are quarantined in a hospital
$\gamma$	The self-healing rate of infected population
$\omega$	The recovered rate of quarantine population
$\delta$	The rate that the recovered population lose immunity
$\tau$	Time delay before the infected population are quarantined in a hospital

**Table 2** Existing confirmed data of COVID-19 released by WHO [2]

Date	Existing confirmed data
January 19	198
January 20	291
January 21	431
January 22	554
January 23	771
January 24	1208
January 25	1870
January 26	2613
January 27	4349
January 28	5739

$$I(t) = e^{(kb-\gamma)t} \tag{4}$$

According to the existing confirmed data of COVID-19 released by WHO, it can be fitted that  $b=0.04133$ . Assuming that a virus carrier closely contacts ten people every day, the infection rate is  $\beta_1 = kb = 0.4133$  in this case (Tables 1 and 2).

During the transmission of infected diseases, the basic regeneration number  $R_0$  is also a crucial factor. In pandemic dynamics, if no isolation measures are taken, Lipsitch et al. have given the simple expression of the basic regeneration number  $R_0 = kbD$  [29]. According to the epidemiological survey results of [30], it is assumed that  $D = 8$ , and by using the case report before January 21, 2020, they estimated the basic regeneration number ( $R_0$ ) of 2019-nCoV to be 3.6–4.0 (95% confidence interval). Cao et al. incorporate human movement data to improve epidemiological estimates for 2019-nCoV, and

they estimate the basic reproduction number to be 3.24 [31]. Basic reproduction number of some highly infectious disease is given in Table 3. Approximately, in this paper, according to the Lipsitch’s method [29], the basic regeneration number  $R_0$  can be calculated as  $R_0 = kbD=3.3064$ .

### 3 Stability of Equilibrium and Bifurcation Analysis

The dynamical behaviors of model (1) proposed in Sect. 2 are studied in this section. An equilibrium of model (1) under which the virus remains pandemics is determined, that is, the equilibrium point. Then, the threshold value of Hopf bifurcation and the stability of the model are studied.

**Theorem 1** *System (1) has a unique positive equilibrium point  $E^* = (S^*, I^*, D^*, Q_1^*, Q_2^*, R^*)$ , where*

$$S^* = \frac{(\gamma + \varphi_2)NI^*}{\beta_1 I^* + \varphi_1 N}, D^* = \varphi_2 \tau I^*, Q_1^* = \frac{N(\gamma + \varphi_2) - \beta_1 S^*}{\beta_2}, Q_2^* = \frac{\varphi_2 I^*}{\omega}, R^* = \frac{(\gamma + \varphi_2)I^*}{\delta}.$$

**Proof** When system (1) is stable, all the derivatives on the left of equal sign of the system are set to zero, which implies that the system becomes stable, it can be obtained:

$$\begin{cases} \delta R(t) - \frac{\beta_1 I(t)S(t)}{N} - \varphi_1 S(t) = 0, \\ \frac{\beta_1 I(t)S(t)}{N} + \frac{\beta_2 I(t)Q_1(t)}{N} - (\gamma + \varphi_2)I(t) = 0, \\ \varphi_2 I(t) - \varphi_2 I(t - \tau) = 0, \\ \varphi_1 S(t) - \frac{\beta_2 I(t)Q_1(t)}{N} = 0, \\ \varphi_2 I(t - \tau) - \omega Q_2(t) = 0, \\ \gamma I(t) + \omega Q_2(t) - \delta R(t) = 0, \end{cases} \tag{5}$$

Since the total number of hosts in system (1) is  $N$ , I can get the following equation of  $I$ ,

**Table 3** Values of  $R_0$  of well-known pandemic diseases

Disease	$R_0$
Chickenpox	10–12 [32]
Pertussis	5.5 [33]
Smallpox	3.5–6 [34]
AIDS	3.65–4.14 [35]
SARS	2–5 [36]
COVID-19	1.4–3.9 [37–40]
Ebola	1.5–2.5 [41]
Seasonal Influenza	0.9–2.1 [42]

$$S^* + I^* + \varphi_2 \tau I^* + \frac{N(\gamma + \varphi_2) - \beta_1 S^*}{\beta_2} + \frac{\varphi_2}{\omega} I^* + \frac{(\gamma + \varphi_2)}{\delta} I^* = N \tag{6}$$

Obviously, Eq. (5) has one unique positive root  $I$ , there is one unique positive equilibrium point  $E^* = (S^*, I^*, D^*, Q_1^*, Q_2^*, R^*)$ . The proof is completed.

According to (2),  $Q_2(t) = N - S(t) - I(t) - D(t) - Q_1(t) - R(t)$ , thus system (1) can be simplified to

$$\begin{cases} \frac{dS(t)}{dt} = \delta R(t) - \frac{\beta_1 I(t)S(t)}{N} - \varphi_1 S(t), \\ \frac{dI(t)}{dt} = \frac{\beta_1 I(t)S(t)}{N} + \frac{\beta_2 I(t)Q_1(t)}{N} - (\gamma + \varphi_2)I(t), \\ \frac{dD(t)}{dt} = \varphi_2 I(t) - \varphi_2 I(t - \tau), \\ \frac{dQ_1(t)}{dt} = \varphi_1 S(t) - \frac{\beta_2 I(t)Q_1(t)}{N}, \\ \frac{dR(t)}{dt} = \gamma I(t) + \omega [N - S(t) - I(t) - D(t) - Q_1(t) - R(t)] - \delta R(t), \end{cases} \tag{7}$$

The Jacobi matrix of system (5) about  $E^* = (S^*, I^*, D^*, Q_1^*, Q_2^*, R^*)$  is given by

$$J(E^*) = \begin{pmatrix} -\frac{\beta_1 I^*}{N} - \varphi_1 & -\frac{\beta_1 S^*}{N} & 0 & 0 & \delta \\ \frac{\beta_1 I^*}{N} & \frac{\beta_1 S^*}{N} + \frac{\beta_2 Q_1^*}{N} - (\gamma + \varphi_2) & 0 & \frac{\beta_2 I^*}{N} & 0 \\ 0 & \theta_2 - \theta_2 e^{-\lambda \tau} & 0 & 0 & 0 \\ \varphi_1 & -\frac{\beta_2 Q_1^*}{N} & 0 & -\frac{\beta_2 I^*}{N} & 0 \\ -\omega & \gamma - \omega & -\omega & -\omega & -\omega - \delta \end{pmatrix} \tag{8}$$

To find the characteristic equation, I have

$$\lambda \mathbf{E} - J(E^*) = \begin{pmatrix} \lambda + \beta_1 a_1 + \varphi_1 & \beta_1 a_2 & 0 & 0 & -\delta \\ -\beta_1 a_1 & \lambda - \beta_1 a_2 - \beta_2 a_3 + \gamma + \varphi_2 & 0 & -\beta_2 a_1 & 0 \\ 0 & -\theta_2 + \theta_2 e^{-\lambda \tau} & \lambda & 0 & 0 \\ -\varphi_1 & \beta_2 a_3 & 0 & \lambda + \beta_2 a_1 & 0 \\ \omega & -\gamma + \omega & \omega & \omega & \lambda + \omega + \delta \end{pmatrix}$$

where  $a_1 = \frac{I^*}{N}, a_2 = \frac{S^*}{N}, a_3 = \frac{Q_1^*}{N}$ . The characteristic equation of that matrix (8) can be obtained by

$$P(\lambda) + Q(\lambda)e^{-\lambda \tau} = 0 \tag{9}$$

The expressions of  $P(\lambda)$  and  $Q(\lambda)$  are

$$P(\lambda) = \lambda^5 + p_4 \lambda^4 + p_3 \lambda^3 + p_2 \lambda^2 + p_1 \lambda + p_0, \quad Q(\lambda) = q_1 \lambda + q_0 \tag{10}$$

where

$$\begin{aligned}
 p_4 &= (\varphi_1 + \omega + \delta + \beta_1 a_1 + \varphi_2 + \beta_2 a_1 + \gamma - \beta_1 a_2 - \beta_2 a_3), \\
 p_3 &= \begin{pmatrix} \varphi_1 \varphi_2 + \omega \varphi_2 + \delta \varphi_2 + \varphi_1 \gamma + \omega \gamma + \delta \gamma \\ + \beta_1 \varphi_2 a_1 + \omega \beta_1 a_1 + \delta \beta_1 a_1 + \varphi_1 \omega + \varphi_1 \delta + \varphi_1 \beta_2 a_1 \\ + \omega \beta_2 a_1 + \delta \beta_2 a_1 + \beta_1 a_1 \gamma + \beta_2 a_1 \gamma + \beta_2 a_1 \varphi_2 + \beta_1 a_1 \beta_2 a_1 \\ - \beta_2 \beta_1 a_1 a_2 - 2 \beta_2 \beta_2 a_1 a_3 - \beta_1 \beta_2 a_1 a_3 \\ - \varphi_1 \beta_1 a_2 - \omega \beta_1 a_2 - \beta_1 \delta a_2 \\ - \varphi_1 \beta_2 a_3 - \omega \beta_2 a_3 - \delta \beta_2 a_3 - \omega \delta \end{pmatrix}, \\
 p_2 &= \begin{bmatrix} ((\omega + \delta) \beta_1 + \beta_2 (\beta_1 a_1 + \varphi_1)) \beta_1 a_1 a_2 \\ + (\omega + \delta) (\beta_1 a_1 + \varphi_1) (\varphi_2 + \gamma + \beta_2 a_1 - \beta_1 a_2 - \beta_2 a_3) \\ + (\varphi_1 + \omega + \delta + \beta_1 a_1) (\varphi_2 - \beta_1 a_2 - 2 \beta_2 a_3 + \gamma) \beta_2 a_1 \\ + \left( \varphi_1 \omega + \beta_1 a_1 \gamma + \omega \beta_1 a_2 + \omega \beta_2 a_3 \right) \delta \\ \left( -\omega \beta_1 a_1 - \beta_2 a_1 \omega - \omega \gamma - \omega \varphi_2 \right) \delta \end{bmatrix}, \\
 p_1 &= \begin{bmatrix} \beta_2 a_1 (\varphi_2 - 2 \beta_2 a_3 + \gamma) (\omega + \delta) (\beta_1 a_1 + \varphi_1) \\ + \delta \beta_2 a_1 (\omega \beta_1 a_2 + \gamma \varphi_1 - \beta_1 a_3 \omega - \varphi_1 \omega - \omega \gamma - \omega \varphi_2) \\ + (\beta_1 a_1 \theta_2 + \gamma \varphi_1 + \varphi_1 \varphi_2 - \beta_1 a_2 \varphi_1 - \beta_2 a_3 \varphi_1) \delta \omega \end{bmatrix}, \\
 p_0 &= (\beta_1 a_1 \gamma + \beta_1 a_1 \omega \theta_2 + \theta_2 \varphi_1 \omega - \beta_1 a_1 \omega) \beta_2 a_1 \delta, \\
 q_1 &= -\beta_1 a_1 \theta_2 \omega \delta, \\
 q_0 &= -(\beta_1 \beta_2 a_1 + \beta_2 \varphi_1) a_1 \theta_2 \omega \delta.
 \end{aligned}$$

**Theorem 2** *If the following conditions (H) hold, then the positive equilibrium  $E^* = (S^*, I^*, D^*, Q_1^*, Q_2^*, R^*)$  is locally asymptotically stable without time delay.*

$$(H): p_4 > 0, p_3 p_4 - p_2 > 0, p_1 + q_1 > 0, p_2 (p_3 p_4 - p_2) - p_4^2 (p_1 + q_1) > 0 \quad (11).$$

**Proof** When  $\tau = 0$ , Eq. (9) simplifies to

$$\lambda^5 + p_4 \lambda^4 + p_3 \lambda^3 + p_2 \lambda^2 + (p_1 + q_1) \lambda + (p_0 + q_0) = 0 \quad (12)$$

According to Routh-Hurwitz criterion, all the roots of Eq. (12) have negative real parts. Hence, I can deduce that the positive equilibrium point  $E^* = (S^*, I^*, D^*, Q_1^*, Q_2^*, R^*)$  is locally asymptotically stable without time delay. The proof is completed.

For Eq. (9), the root is  $\lambda = i\alpha (\alpha > 0)$ , which was substituted into Eq. (9). After separating the real and imaginary parts, two equations were obtained:

$$p_4 \alpha^4 - p_2 \alpha^2 + p_0 + q_1 \alpha \sin(\alpha \tau) + q_0 \cos(\alpha \tau) = 0 \quad (13)$$

$$\alpha^5 - p_3 \alpha^3 + p_1 \alpha + q_1 \alpha \cos(\alpha \tau) - q_0 \sin(\alpha \tau) = 0 \quad (14)$$

Uniting Eq. (13) and (14), Eq. (15) is obtained:

$$q_1^2 \alpha^2 + q_0^2 = (p_4 \alpha^4 - p_2 \alpha^2 + p_0)^2 + (\alpha^5 - p_3 \alpha^3 + p_1 \alpha)^2 \quad (15)$$

which implies



$$\begin{aligned} &\alpha^{10} + (p_4^2 - 2p_3)\alpha^8 + (p_3^2 + 2p_1 - 2p_2p_4)\alpha^6 \\ &+ (2p_0p_4 + p_2^2 - 2p_1p_3)\alpha^4 \\ &+ (p_1^2 - 2p_0p_2 - q_1^2)\alpha^2 + p_0^2 - q_0^2 = 0, \end{aligned}$$

that is

$$\alpha^{10} + D_4\alpha^8 + D_3\alpha^6 + D_2\alpha^4 + D_1\alpha^2 + D_0 = 0 \tag{16}$$

where

$$\begin{aligned} D_4 &= p_4^2 - 2p_3, \\ D_3 &= p_3^2 + 2p_1 - 2p_2p_4, \\ D_2 &= 2p_0p_4 + p_2^2 - 2p_1p_3, \\ D_1 &= p_1^2 - 2p_0p_2 - q_1^2, \\ D_0 &= p_0^2 - q_0^2. \end{aligned} \tag{17}$$

Let  $x = \alpha^2$ , then Eq. (16) can be turned into:

$$f(x) = x^5 + D_4x^4 + D_3x^3 + D_2x^2 + D_1x + D_0 = 0 \tag{18}$$

Let us assume that the following conditions  $(H_1)$  hold:  $p_4 > 0, d_1 > 0, p_1 > 0, p_2d_1 - p_4^2p_1 > 0$  is satisfied. From previous derivation, Eq. (18) has at least a positive root  $\alpha_0$  which also means Eq. (9) has a pair of purely imaginary roots  $\pm i\alpha_0$ . By uniting Eq. (13) and Eq. (14), the corresponding threshold value  $\tau_k > 0$  can be gotten:

$$\tau_k = \frac{1}{\alpha_0} \arccos \left[ \frac{q_0(p_2\alpha_0^2 - p_4\alpha_0^4 - p_0) + q_1\alpha_0(p_3\alpha_0^3 - \alpha_0^5 - p_1\alpha_0)}{q_0^2 + q_1^2\alpha_0^2} \right] + \frac{2k\pi}{\alpha_0} \tag{19}$$

Let  $\lambda(\tau) = \nu(\tau) + i\omega(\tau)$  be the root of Eq. (9). It is satisfied that  $\nu(\tau_k) = 0, \omega(\tau_k) = \alpha_0$  when  $\tau = \tau_k$ .

**Theorem 3** *Supposing  $f'(x_0) \neq 0$ . If  $\tau = \tau_k$ , and  $\pm i\alpha_0$  is a pair of purely imaginary roots of Eq. (9), then  $\frac{d\text{Re}\lambda(\tau_k)}{d\tau} > 0$ .*

**Proof** This means that there exists at least one eigenvalue with positive real part when  $\tau > \tau_k$ . Differentiating on both sides of Eq. (9) with respect to  $\tau$ , I can obtain:

$$\begin{aligned} \left(\frac{d\lambda}{d\tau}\right)^{-1} &= \frac{(5\lambda^4 + 4p_4\lambda^3 + 3p_3\lambda^2 + 2p_2\lambda + p_1) + q_1e^{-\lambda\tau} - (q_1\lambda + q_0)\tau e^{-\lambda\tau}}{(q_1\lambda + q_0)\lambda e^{-\lambda\tau}} \\ &= \frac{(5\lambda^4 + 4p_4\lambda^3 + 3p_3\lambda^2 + 2p_2\lambda + p_1)e^{\lambda\tau}}{(q_1\lambda + q_0)\lambda} + \frac{q_1}{(q_1\lambda + q_0)\lambda} - \frac{\tau}{\lambda} \end{aligned} \tag{20}$$

Then,

$$\begin{aligned} \operatorname{sgn}\left[\frac{d\operatorname{Re}\lambda}{d\tau}\right]_{\tau=\tau_k} &= \operatorname{sgn}\left[\operatorname{Re}\left(\frac{d\lambda}{d\tau}\right)^{-1}\right]_{\lambda=i\alpha_0} \\ &= \operatorname{sgn}\left[\operatorname{Re}\left(\frac{(5\lambda^4 + 4p_4\lambda^3 + 3p_3\lambda^2 + 2p_2\lambda + p_1)e^{\lambda\tau}}{(q_1\lambda + q_0)\lambda} + \frac{q_1}{(q_1\lambda + q_0)\lambda} - \frac{\tau}{\lambda}\right)\right]_{\lambda=i\alpha_0} \\ &= \operatorname{sgn}\frac{4\alpha_0^6 + (3p_4^2 - 6p_3)\alpha_0^4 + (2p_3^2 + 4p_1 - 4p_2p_4)\alpha_0^2 + (p_2^2 + 2p_0p_4 - 2p_1p_3)}{q_1^2\alpha_0^2 + q_0} \\ &= \operatorname{sgn}\{f'(\alpha_0^2)\} \end{aligned}$$

It follows that  $f'(x_0) \neq 0$ , therefore,

$$\left.\frac{d(\operatorname{Re}\lambda)}{d\tau}\right|_{\tau=\tau_k} > 0. \tag{21}$$

According to Routh’s theorem [43], as  $\tau$  continuously varies from a value less than  $\tau_k$  to one greater than  $\tau_k$ , the root of characteristic Eq. (9) crosses from left to right on the imaginary axis. Thus, the transverse condition holds and the conditions for Hopf bifurcation are satisfied at  $\tau = \tau_k$  according to Hopf bifurcation theorem. Therefore, the following conclusions can be obtained.

**Theorem 4** *Supposing that the conditions  $(H_1)$  are satisfied.*

- (1) When  $0 \leq \tau < \tau_0$ , the positive equilibrium  $E^* = (S^*, I^*, D^*, Q_1^*, Q_2^*, R^*)$  of system (2) is locally asymptotically stable, and unstable when  $\tau \geq \tau_0$ .
- (2) If Eq. (9) has a pair of purely imaginary roots  $\pm i\alpha_0$ , the system undergoes a Hopf bifurcation at the positive equilibrium  $E^* = (S^*, I^*, D^*, Q_1^*, Q_2^*, R^*)$  when time delay  $\tau = \tau_0$ .

This implies that when time delay  $\tau < \tau_0$ , the system will stabilize at the equilibrium point, which is beneficial for us to implement a containment strategy; when the delay  $\tau \geq \tau_0$ , the system will be unstable and the virus cannot be effectively controlled.

## 4 Numerical Simulations

In this section, numerical simulations are conducted to reveal the pandemic dynamics of COVID-19, and some nonlinear properties of the system are verified. In the following experiments, it is assumed that the total number of population is 10000000, at the beginning, the number of infected population is 10. And I will conduct experiments in two cases, with  $\tau < \tau_0$  and  $\tau \geq \tau_0$ .

### 4.1 The Case of $\tau < \tau_0$

The value of parameters is listed as follows.

Because the population at home isolation state contact fewer people, the infection rate for home isolation population ( $\beta_2$ ) is lower than the infection rate for susceptible

population ( $\beta_1$ ). Assuming that they contact eight people every day, the infection rate for home isolation population is  $\beta_2 = kb = 0.33064$  in this case. Currently, the duration of medical observation before hospital quarantine is generally 14 days, it means that the delay time can be 14 days in this case. When  $\tau = 14 < \tau_0$ , we can see the changes of the numbers of six states of population in Fig. 2. It can be found that the equilibrium point  $E^* = (S^*, I^*, D^*, Q_1^*, Q_2^*, R^*)$  is locally asymptotically stable.

The parameter  $\varphi_2$  indicates the intensity of isolation policy. In other words, larger parameters  $\varphi_2$  mean that the hospital can treat more patients. It has a direct impact on the number of infected population. Figure 3 shows the change of the infected population with different  $\varphi_2$  when  $\tau = 14 < \tau_0$ . Obviously, increasing the intensity of hospital quarantine can significantly improve the effect of pandemic control. In other words, the government should increase the number of tested people with or without symptoms in order to identify early on clusters of infection which can be targeted with an isolation strategy.

### 4.2 The Case of $\tau \geq \tau_0$

The delay will increase as the incubation period increases. Once the delay exceeds the threshold value, the pandemic dynamic system is at risk of instability. The stability of equilibrium point is simulated when  $\tau=40 \geq \tau_0$  in Fig. 4. The values of parameters are the same as in Table 1 except  $\tau$ . The equilibrium is unstable within 1000 days. To show the stability of equilibrium point when  $\tau=40$  more clearly, the number of infected population  $I(t)$

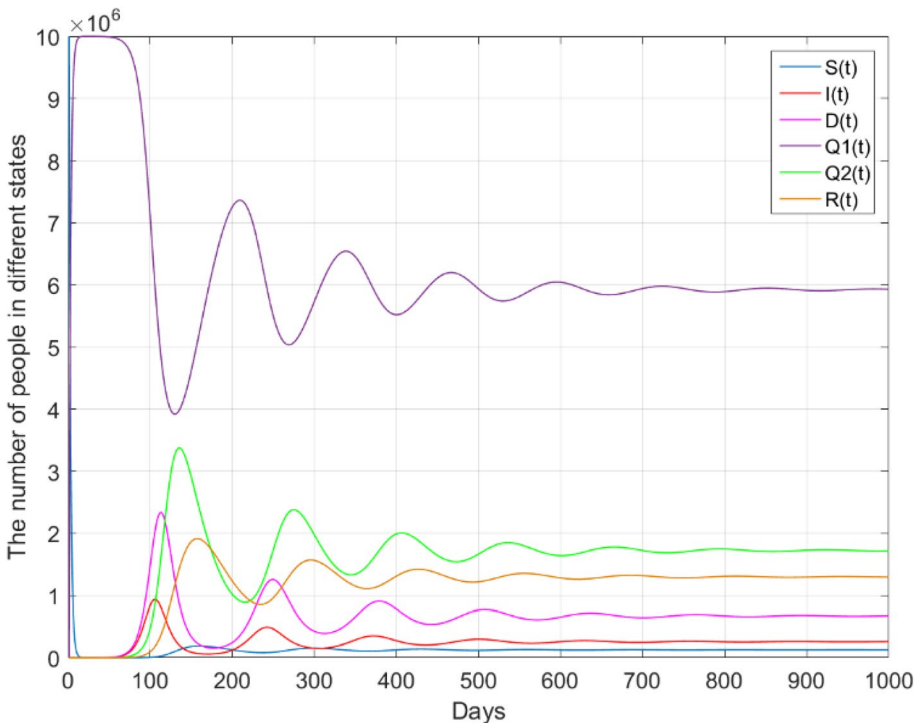
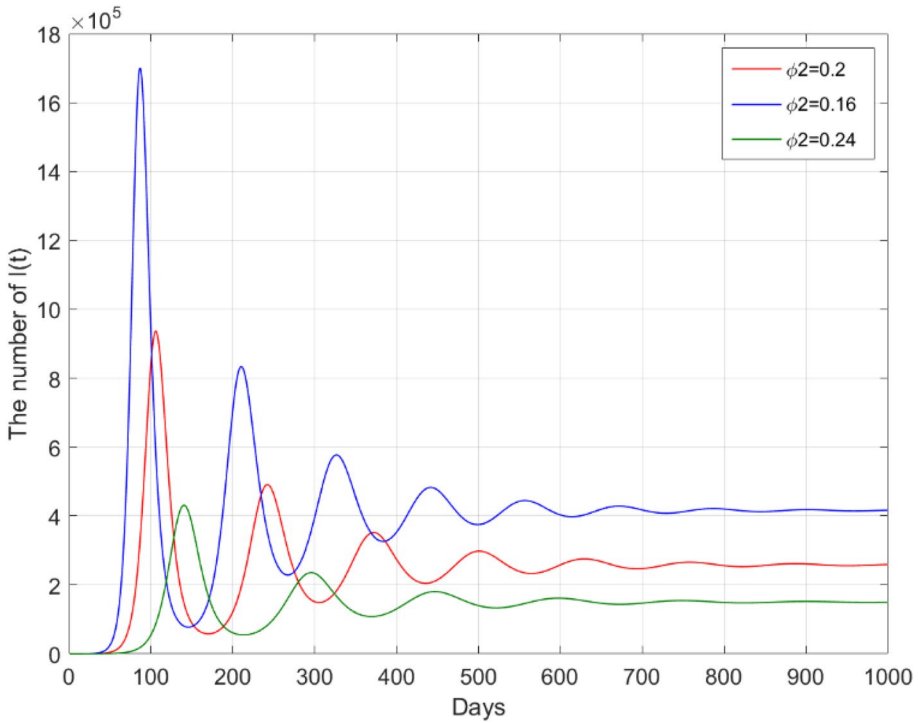


Fig. 2 Equilibrium for the pandemic mode when  $\tau = 14 < \tau_0$



**Fig. 3** The number of infected population  $I(t)$  with different  $\phi_2$

with different  $\beta_2$  is shown in Fig. 5 on a larger time scale. For the same virus (COVID-19), the change in infectious ability is very small. For  $\beta_2 = kb$ , the number of people that the population at home isolation state contact each day ( $k$ ) is the key factor. In Fig. 5, three cases ( $k = 6, 8, 10$ , correspondingly,  $\beta_2 = 0.24798, 0.33064, 0.4133$ ) are shown. When  $\beta_2 = \beta_1 = 0.4133$ , it can clearly find that the number of infected population will outburst after a short period of peace and repeat again and again. In this situation, the effect of home isolation fails. When the population at home isolation state contact two people less every day ( $\beta_2 = 0.24798, 0.33064$ ), the effect of home isolation is very significant. This illustrates the importance of home isolation for pandemic control, it is crucial that residents restrain their daily behavior, and it is a feasible solution for pandemic prevention (Table 4).

The annual, biennial or sporadic COVID-19 outbreak is similar to the projection of the researchers in Harvard University which was published in *Science*. They project that if the immunity of the antibody maintains for 40 weeks or 104 weeks, it will favor annual COVID-19 outbreaks or biennial outbreaks [44]. Obviously, the term of immunity affects the parameters  $\delta$  in the model, then the simulation with different  $\delta$  is shown in Fig. 6.

In Figs. 6 and 7, the influence of the rate  $\delta$  and the self-healing rate  $\gamma$  on the spread of the virus is simulated, respectively. From the two figures, we can find that lower  $\delta$  and larger  $\gamma$  are more beneficial for the prevention of COVID-19. It means that we should improve the self-healing ability of infected population and maintain the immunity of the recovered population (vaccine may be the best method). In other words, the longer the vaccine effect lasts, the easier it is to limit the spread of the virus.

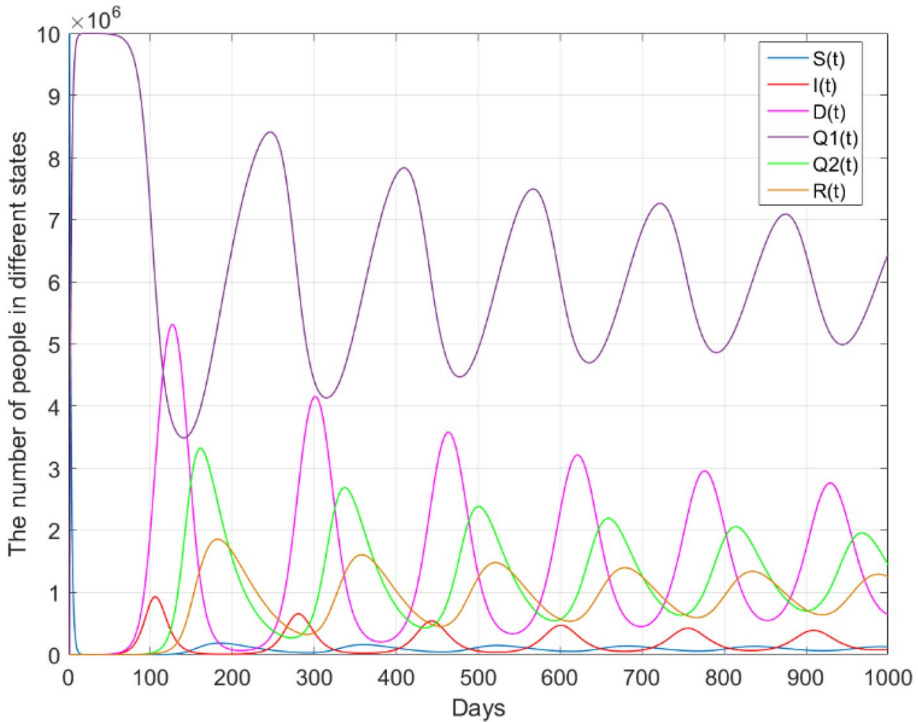


Fig. 4 Equilibrium for the pandemic mode when  $\tau = 40 \geq \tau_0$

### 4.3 Hopf Bifurcation of the Equilibrium

To show the bifurcation phenomenon of the equilibrium clearly in the model, the results of numerical experiment are shown in Figs. 8, 9, 10, 11 and 12. Figure 8 shows the projection of the phase portrait in  $(I, Q, R)$ -space when  $\tau = 40$ , the value of parameters is listed in Table 5. The curve radiates to a limit cycle which implies the system is unstable, and it corresponds to the curve  $(\beta_2 = 0.4133)$  in Fig. 5. Then, let us observe the effect of  $\beta_2$  and  $\delta$  on the bifurcation phenomenon in Figs. 9 and 10, respectively. In Fig. 9, only the infection rate for home isolation population ( $\beta_2$ ) is decreased, then it is found that the curve converges to a fixed point which implies the system is stable. In Fig. 10, only the rate  $\delta$  is decreased, and the curve converges to a fixed point which implies the system is stable as well. It means that the parameters  $\beta_2$  and  $\delta$  affect the threshold  $\tau_0$  of bifurcation.

Figure 11 gives the bifurcation diagram of the equilibrium with the parameters  $\beta_2=0.4133, \delta = 0.04$ . It can be easily obtained that the Hopf bifurcation occurs at about  $\tau = \tau_0 = 33$  which is similar to the results of theoretical derivation. Figure 12 gives the bifurcation diagram of the equilibrium with the parameters  $\beta_2=0.33064, \delta = 0.02$ . The Hopf bifurcation occurs at about  $\tau = \tau_0 = 43$ . Comparing the two Figs, it shows that the parameters  $\beta_2$  and  $\delta$  have effect on the time that Hopf bifurcation occurs. As the parameters  $\beta_2$  and  $\delta$  decrease, the threshold value of the bifurcation increases, and the control of the pandemic is more effective. This confirms the importance of home isolation and the immunity of the population (or the vaccine effect) once again.

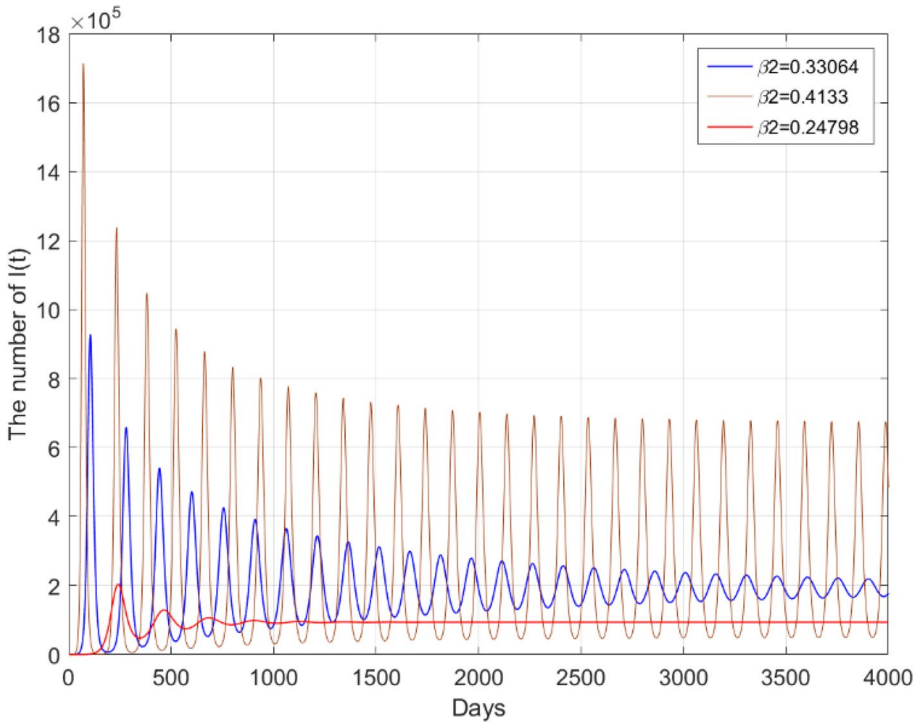


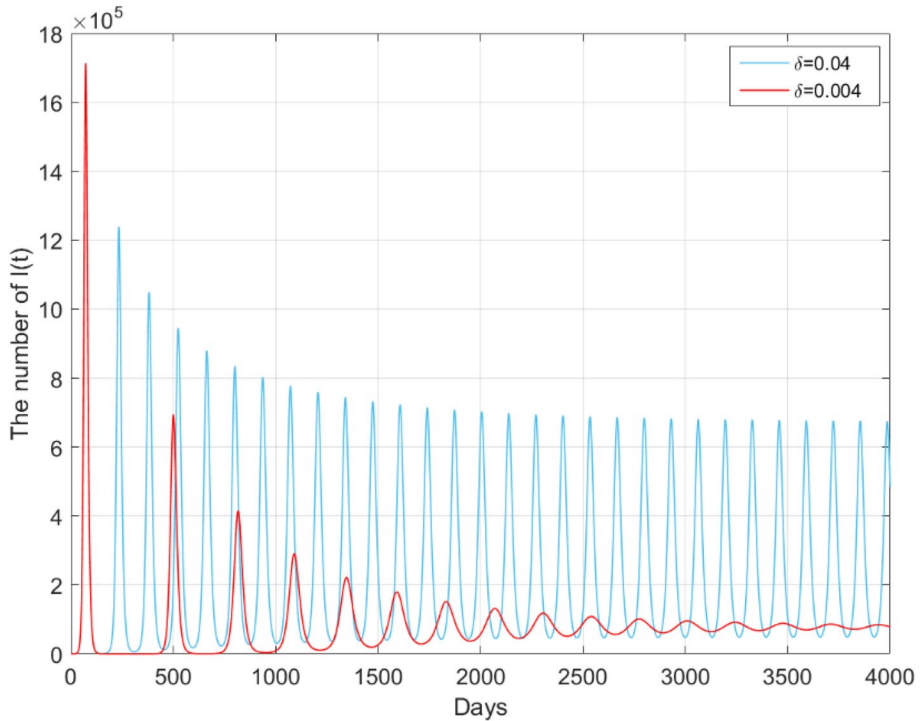
Fig. 5 The number of infected population  $I(t)$  with different  $\beta_2$  when  $\tau = 40$

Table 4 Parameters in the simulations

Notations	Value
$\beta_1$	0.4133
$\beta_2$	0.33064
$\varphi_1$	0.4
$\varphi_2$	0.2
$\gamma$	0.001
$\omega$	0.03
$\delta$	0.04
$\tau$	14

### 5 Discussion and Conclusion

In the proposed model, hierarchical quarantine strategy is deployed to prevent the COVID-19 outbreak, and home isolation is a feasible and crucial measure. To illuminate the role of home isolation in the pandemic prevention, a simplified model without the home isolation state is proposed to compare with the hierarchical quarantine strategy. The transition diagram is given in Fig. 13. And the value of the parameters is the same as that in Table 4. The case of  $\tau = 14 < \tau_0$  is conducted to show the comparison. The number of infected



**Fig. 6** The number of infected population  $I(t)$  with different  $\delta$  when  $\tau = 40$ ,  $\beta_2 = \beta_1 = 0.4133$

population is shown in Fig. 14. The effect of home isolation is clearly shown in Fig. 14. When the dynamic system reaches the equilibrium point, the number of infected population without home isolation is larger than that with hierarchical quarantine strategy. In addition, the peak in the model with hierarchical quarantine strategy is much lower than that without home isolation. The result indicates that the hierarchical quarantine strategy can inhibit the spread of COVID-19 effectively. The surveillance of COVID-19 should be maintained as normal and people should restrain their actions at this urgent time and try to avoid close contact with people as much as possible.

In summary, a pandemic model with hierarchical quarantine and time delay is developed for the COVID-19 outbreak. Time delay caused by virus incubation period and the possibility of reinfection due to antibody failure are well considered in the model. The model gives a better description of the spread of COVID-19 and some suggestions worth considering for the COVID-19 prevention. For example, the government should increase the number of tested people with or without symptoms in order to identify early on clusters of infection which can be targeted with an isolation strategy. The stability of the equilibrium and the bifurcation phenomenon is analyzed in detail. The threshold value  $\tau_k$  of the bifurcation is deduced and quantitatively analyzed. When the time delay

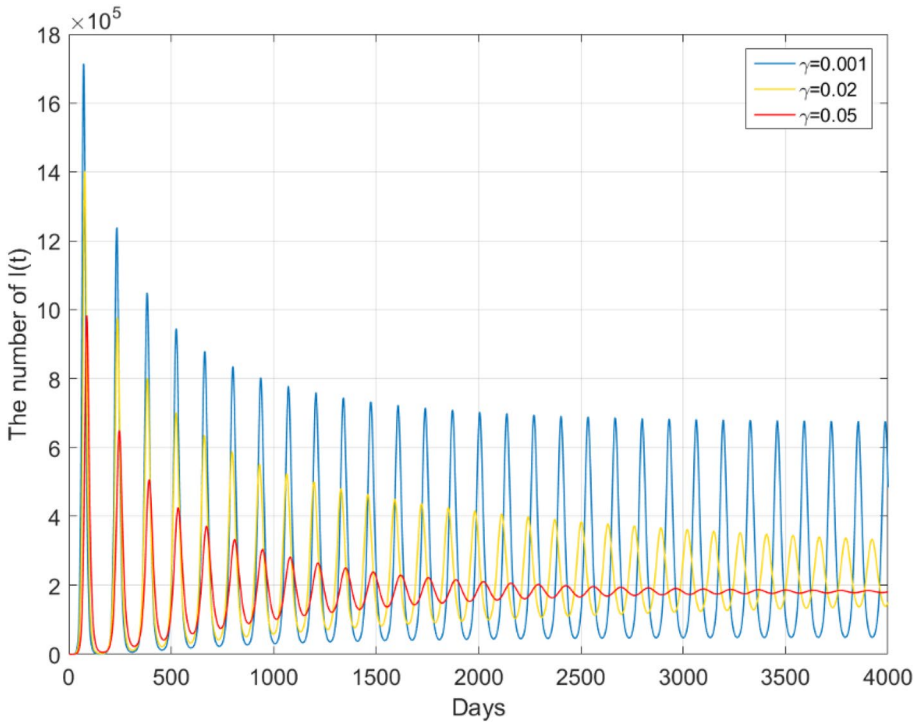


**Fig. 7** The number of infected population  $I(t)$  with different  $\gamma$  when  $\tau = 40, \beta_2 = \beta_1 = 0.4133$

is low, i.e.,  $\tau < \tau_0$ , the system will stabilize at the equilibrium point, which is beneficial for us to implement a containment strategy of COVID-19; when the time delay is long, i.e.,  $\tau \geq \tau_0$ , the system will be unstable and the virus cannot be effectively controlled. Fortunately, the simulations show that the COVID-19 pandemic dynamic system is stable with  $\tau=14$  (at present, the latent observation period is usually two weeks), however, the trend of the COVID-19 pandemic may have some ups and downs in a period of time. In addition, the results of the numerical simulations show that lower  $\delta$  (larger self-healing rate) and larger  $\gamma$  (vaccine with better immunogenicity) are more beneficial for pandemic prevention of COVID-19,  $\delta$  means the rate that the recovered population lose immunity, and  $\gamma$  means the self-healing rate of infected population. If the immunity of recovered population lasts for a short time, the prevention of COVID-19 will be beset with difficulties. Evidently, home isolation is a more feasible and effective measure. The simulations show that a lower  $\beta_2$  can expand the threshold  $\tau_0$  of bifurcation, which leads a better effect of the COVID-19 prevention. For the public, just staying home and avoiding close contact with people will provide great support to prevent the COVID-19 outbreak.



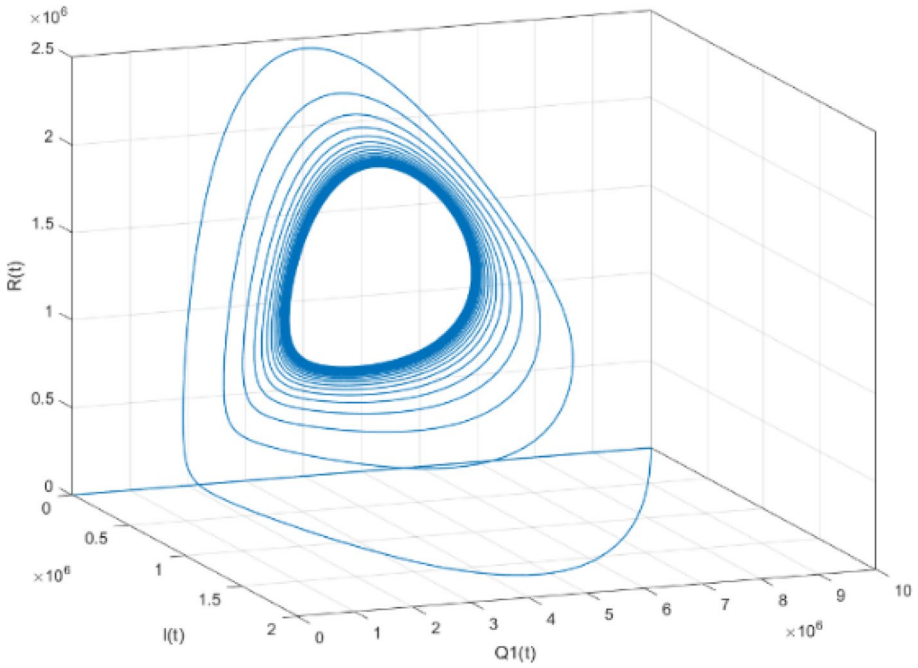


**Fig. 8** The projection of the phase portrait in  $(I, Q_1, R)$ -space when  $\beta_2=0.4133, \delta = 0.04$

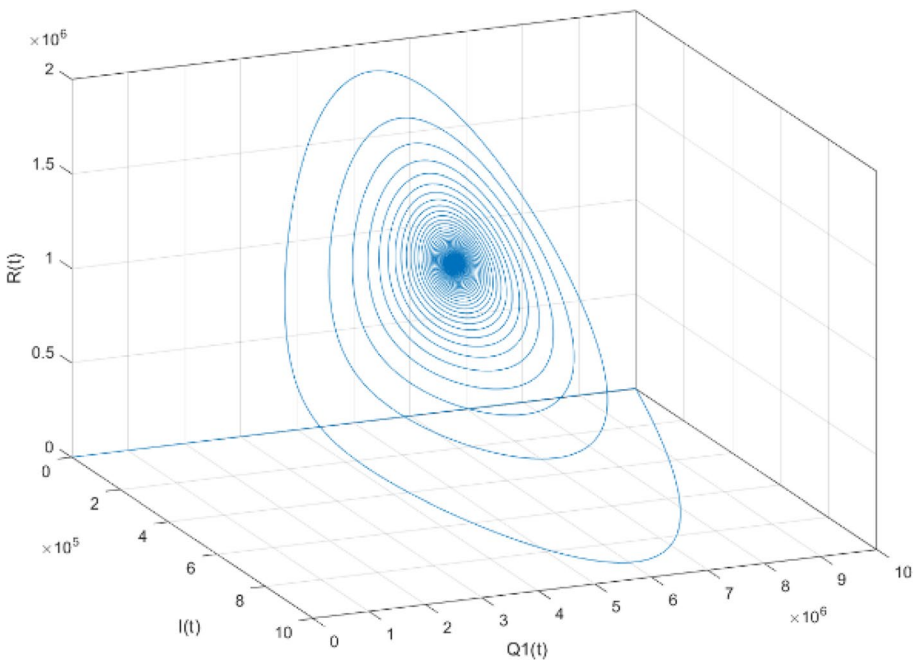


**Fig. 9** The projection of the phase portrait in  $(I, Q_1, R)$ -space when  $\beta_2 = 0.33064, \delta = 0.04$

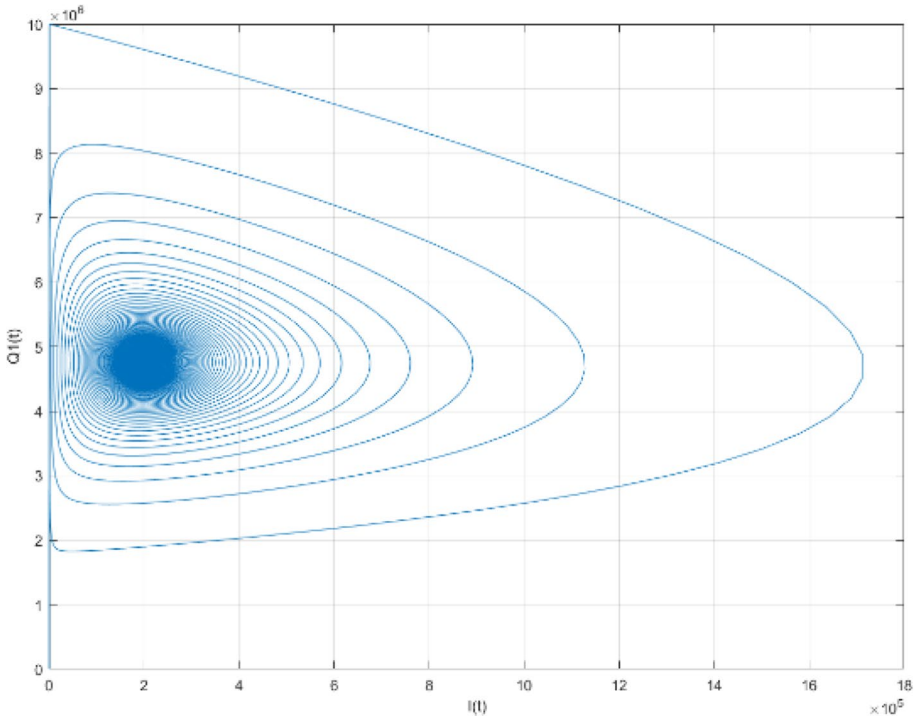


**Fig. 10** The phase portrait of  $Q_1(t)$  and  $I(t)$  when  $\beta_2=0.4133, \delta = 0.02$

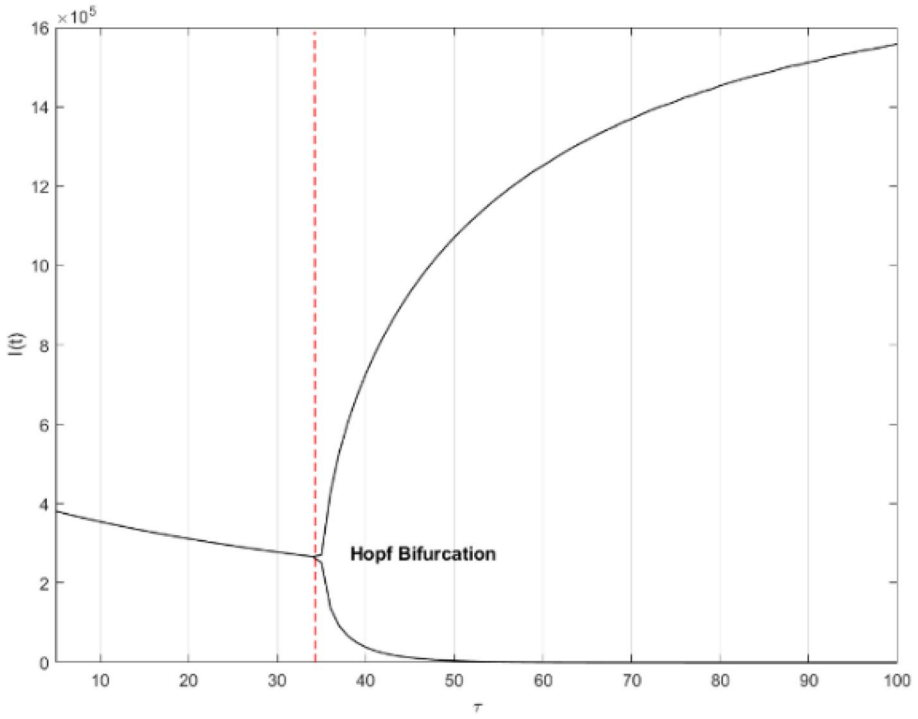


Fig. 11 Bifurcation diagram of the equilibrium with  $\beta_2=0.4133, \delta = 0.04$

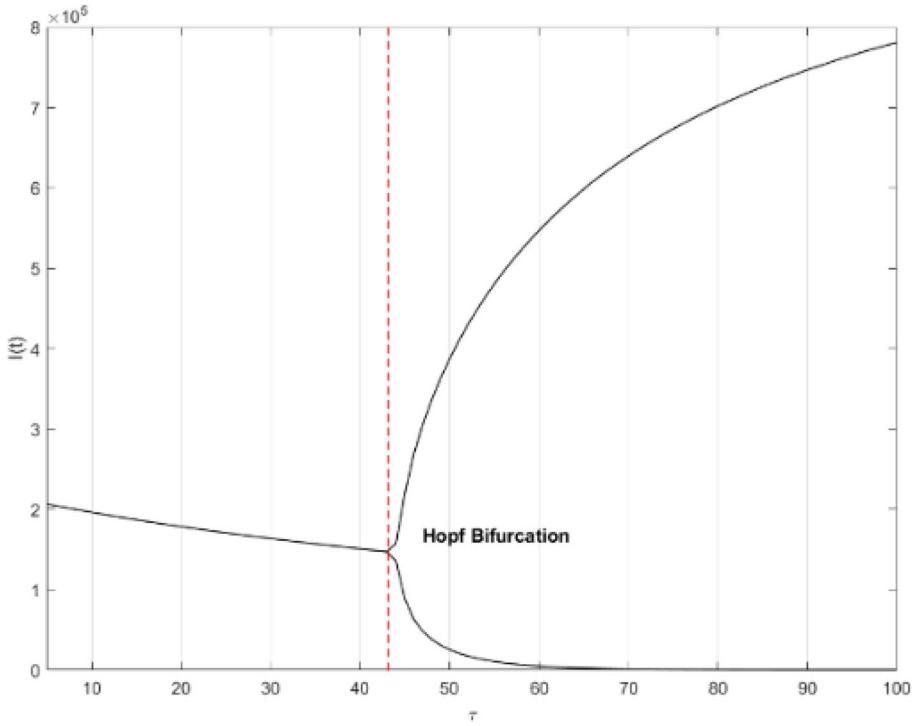
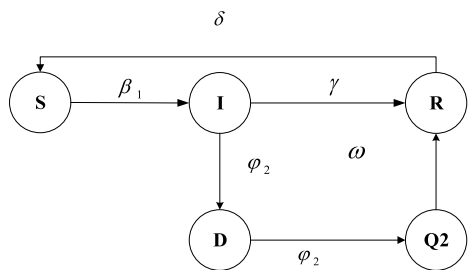


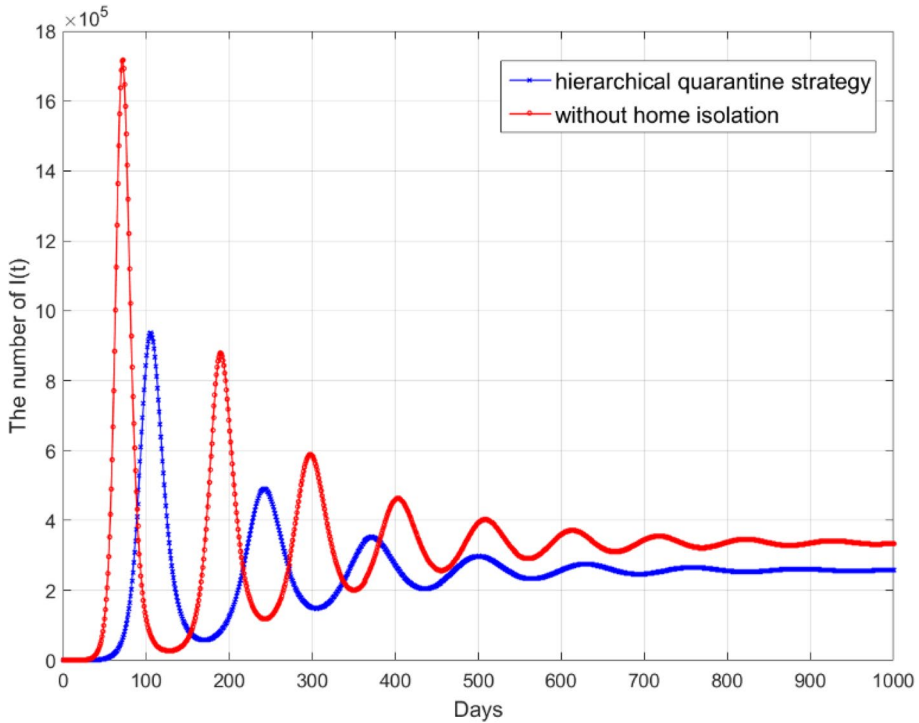
Fig. 12 Bifurcation diagram of the equilibrium with  $\beta_2=0.33064, \delta = 0.02$

Table 5 Parameters in Fig. 9

Notations	Value
$\beta_1$	0.4133
$\beta_2$	0.4133
$\varphi_1$	0.4
$\varphi_2$	0.2
$\gamma$	0.001
$\omega$	0.03
$\delta$	0.04
$\tau$	40

Fig. 13 State transition diagram of the pandemic model without home isolation





**Fig. 14** Comparison of the infected population for the two models

**Acknowledgements** This work was supported by the Key Research and Development Program of Liaoning Province under Grant No. 2019JH2/10100019 and Fundamental Research Funds for the Central Universities under Grant No. N181606001, N2016011 and N2024005-1. It is also funded by the China National Study Abroad Fund.

#### Declaration

**Conflict of interest** I declare that there is no conflict of interest regarding the publication of this paper.

## References

1. Tyrrell DA, Bynoe ML (1966) Cultivation of viruses from a high proportion of patients with colds. *Lancet* 287(7248):76–77
2. <https://www.who.int/emergencies/diseases/novel-coronavirus-2019/events-as-they-happen>
3. Hamer WH (1906) Epidemic disease in England—the evidence of variety and of persistency of type. *Lancet* 1(4305):733–739
4. Ross R (1911) *The prevention of malaria*. Murray, London
5. Kermack WO, McKendrick AG (1927) Contributions to the mathematical theory of epidemics. *Proc R Soc London Series A* 115(772):700–721
6. Dalal N, Greenhalgh D, Mao X (2007) A stochastic model of AIDS and condom use. *J Math Anal Appl* 325(1):36–53

7. Gray A, Greenhalgh D, Hu L, Mao X, Pan J (2011) A stochastic differential equation SIS epidemic model. *SIAM J Appl Math* 71(3):876–902
8. Lahrouz A, Omari L, Kiouach D (2011) Global analysis of a deterministic and stochastic nonlinear SIRS epidemic model. *Nonlinear Anal Model Control* 16:59–76
9. Tornatore E, Buccellato SM, Vetro P (2005) Stability of a stochastic SIR system. *Phys A* 354:111–126
10. Chowell G, Sattenspiel L, Bansal S, Viboud C (2016) Mathematical models to characterize early epidemic growth: a Review. *Phys Life Rev* 18:66–97
11. Stehle J, Voirin N, Barrat A et al (2011) Simulation of an SEIR infectious disease model on the dynamic contact network of conference attendees. *BMC Med* 9:87
12. Chan JF, Zhang AJ, Yuan S, Poon VK et al (2020) Simulation of the clinical and pathological manifestations of coronavirus disease 2019 (COVID-19) in golden Syrian hamster model: implications for disease pathogenesis and transmissibility. *Clin Infect Dis*. <https://doi.org/10.1093/cid/ciaa325>
13. Tian J, Wu J, Bao Y et al (2020) Modeling analysis of COVID-19 based on morbidity data in Anhui, China. *Math Biosci Eng* 17:2842–2852
14. Dai C, Yang J, Wang K (2020) Evaluation of prevention and control interventions and its impact on the epidemic of coronavirus disease 2019 in Chongqing and Guizhou Provinces. *Math Biosci Eng* 17(4):2781–2791
15. Prem K, Liu Y, Russell TW, Kucharski AJ, Eggo RM, Davies N (2020) Centre for the mathematical modelling of infectious diseases COVID-19 working group, the effect of control strategies to reduce social mixing on outcomes of the COVID-19 epidemic in Wuhan, China: a modelling study. *Lancet F Health*. [https://doi.org/10.1016/S2468-2667\(20\)30073-6](https://doi.org/10.1016/S2468-2667(20)30073-6)
16. Zhao S, Chen H (2020) Modeling the epidemic dynamics and control of COVID-19 outbreak in China. *Quant Biol* 8:11–19
17. Tang B, Bragazzi NL, Li Q, Tang S, Xiao Y, Wu J (2020) An updated estimation of the risk of transmission of the novel coronavirus (2019-nCoV). *Infect Dis Model* 5:248–255
18. Chen TM, Rui J, Wang QP, Zhao ZY, Cui JA, Yin L (2020) A mathematical model for simulating the phase-based transmissibility of a novel coronavirus. *Infect Dis Poverty* 9(1):24–24
19. Wang H, Wang Z, Dong Y (2020) Phase-adjusted estimation of the number of coronavirus disease 2019 cases in Wuhan, China. *Cell Discov*. <https://doi.org/10.1038/s41421-020-0148-0>
20. Sun T, Weng D (2020) Estimating the effects of asymptomatic and imported patients on COVID-19 epidemic using mathematical modeling. *J Med Virol* 92(10):1995–2003
21. Shao P, Shan Y (2020) Beware of asymptomatic transmission: Study on 2019 nCoV prevention and control measures based on extended SEIR model. *bioRxiv*
22. Li L (2015) Bifurcation and chaos in a discrete physiological control system. *Appl Math Comput* 252:397–404
23. Din Q (2017) Global stability and Neimark-Sacker bifurcation of a host-parasitoid model. *Int J Syst Sci* 48(6):1194–1202
24. Huang C, Cao J, Xiao M, Alsaedi A, Hayat T (2017) Bifurcations in a delayed fractional complex-valued neural network. *Appl Math Comput* 292:210–227
25. Dong T, Liao X, Li H (2012) Stability and hopf bifurcation in a computer virus model with multistate antivirus. *Abstr Appl Anal* 2012:1–16
26. Ren J, Yang XF, Yang LX (2012) A delayed computer virus propagation model and its dynamics. *Chaos Solitons Fractals* 45(1):74–79
27. Wang S, Liu QM, Yu XF (2010) Bifurcation analysis of a model for network worm propagation with time delay. *Math Comput Model* 52(3):435–447
28. Zhu Q, Yang XF, Ren J (2012) Modeling and analysis of the spread of computer virus. *Commun Nonlinear Sci Numer Simul* 17(12):5117–5124
29. Lipsitch M, Cohen T, Cooper B et al (2003) Transmission dynamics and control of severe acute respiratory syndrome. *Science* 300(5627):1966–1970
30. Chan JF, Yuan S, Kok K et al (2020) A familial cluster of pneumonia associated with the 2019 novel coronavirus indicating person-to-person transmission: a study of a family cluster. *Lancet* 395(10223):514–523
31. Cao Z, Zhang Q, Lu X et al (2020) Incorporating human movement data to improve epidemiological estimates for 2019-nCoV. *MedRxiv* 362:170
32. Ireland's Health Services (2020) Health Care Worker Information (PDF). Retrieved March 27
33. Kretzschmar M, Teunis PF, Pebody RG (2010) Incidence and reproduction numbers of pertussis: estimates from serological and social contact data in five European countries. *PLOS Med* 7(6):1000291
34. Gani R, Leach S (2001) Transmission potential of smallpox in contemporary populations. *Nature* 414(6865):748–751

35. Nishiura H (2010) Correcting the actual reproduction number: a simple method to estimate  $R_0$  from early epidemic growth data. *Int J Environ Res Public Health* 7(1):291–302
36. Wallinga J, Teunis P (2004) Different epidemic curves for severe acute respiratory syndrome reveal similar impacts of control measures. *Am J Epidemiol* 160(6):509–516
37. Riou J, Althaus CL (2020) Pattern of early human-to-human transmission of Wuhan 2019 novel coronavirus (2019-nCoV), December 2019 to January 2020. *Eurosurveillance* 25(4):2000058
38. Liu T, Hu J, Kang M, Lin L (2020) Time-varying transmission dynamics of novel coronavirus pneumonia in China. *bioRxiv* 2: 79
39. Read JM, Bridgen JR, Cummings DA et al (2020) Novel coronavirus 2019-nCoV: early estimation of epidemiological parameters and epidemic predictions. *MedRxiv* 10(7):1258
40. Wu JT, Leung K, Bushman M et al (2020) Estimating clinical severity of COVID-19 from the transmission dynamics in Wuhan, China. *Nat Med* 26(4):506–510
41. Althaus CL (2014) Estimating the reproduction number of ebola virus (EBOV) during the 2014 outbreak in West Africa. *PLOS Curr*. <https://doi.org/10.1371/currents.outbreaks.91afb5e0f279e7f29e7056095255b288>
42. Coburn BJ, Wagner BG, Blower S (2009) Modeling influenza epidemics and pandemics: insights into the future of swine flu (H1N1). *BMC Med* 7(1):30–30
43. Hassard B, Kazarino D, Wan Y (1981) Theory and application of Hopf bifurcation. Cambridge University Press, Cambridge, pp 210–211
44. Kissler SM, Tedijanto C, Goldstein E et al (2020) Projecting the transmission dynamics of SARS-CoV-2 through the post epidemic period. *Science* 368:860–868
45. Fu X, Small M, Chen G (2014) Propagation dynamics on complex networks: models, methods and stability analysis. Higher Education Press, Beijing

**Publisher's Note** Springer Nature remains neutral with regard to jurisdictional claims in published maps and institutional affiliations.